

Electronic Supplementary Information

Hierarchical ZSM-5 with Tunable Structure and Enhanced Mass

Diffusion

Xuan Wu,^{a, #} Bojun Zeng,^{a, #} Siming Wu,^{a, *, #} Lu Wu^a, Liang Mao^a, Yitian Wang^a, Fengjuan Wu^a, Ge Tian,^{a, *}
Liyang Wang^c, Ganggang Chang^a, Christoph Janiak^d, and Xiaoyu Yang^{a, b, *}

contents

1. Materials and Methods	1
1.1 Chemicals and Reagents	1
1.2 Synthesis	1
1.3 Characterization	2
1.4 Catalytic Evaluation	3
2. Supplementary Figures and Tables	4
3. References	27

1. Materials and Methods

1.1 Chemicals and Reagents

All chemicals and reagents are supplied by commercial suppliers and used without further purification: tetraethyl orthosilicate (TEOS, 98%, Shanghai Aladdin Biochemical Technology Co, Ltd.), silica gel (Davisil Grade 635, Shanghai Aladdin Biochemical Technology Co, Ltd.), colloidal silica (LUDOX HS-40, 40 wt. % suspension in water, Shanghai Aladdin Biochemical Technology Co. Ltd.), sodium aluminate (NaAlO_2 , 98%, technical, Shanghai Aladdin Biochemical Technology Co, Ltd.), aluminum isopropoxide ($\text{Al}(\text{i-PrO})_3$, 98%, Shanghai Aladdin Biochemical Technology Co. Ltd.), aluminium hydroxide ($\text{Al}(\text{OH})_3$, 99.99%, Shanghai Aladdin Biochemical Technology Co. Ltd.), aluminum sulfate octadecahydrate ($\text{Al}_2(\text{SO}_4)_3 \cdot 18\text{H}_2\text{O}$, AR, 99%, Shanghai Aladdin Biochemical Technology Co. Ltd.), aluminium chloride hexahydrate ($\text{AlCl}_3 \cdot 6\text{H}_2\text{O}$, AR, Sinopharm Chemical Reagent Co. Ltd.), sodium chloride (NaCl , 99.5%, Sinopharm Chemical Reagent Co. Ltd.), sodium hydroxide (NaOH , 96%, Sinopharm Chemical Reagent Co. Ltd.), tetrabutylammonium hydroxide (TBAOH, AR, 40 wt. % in water, Shanghai Aladdin Biochemical Technology Co, Ltd.), tetraethylammonium hydroxide (TEAOH, AR, 25 wt. % in water, Shanghai Aladdin Biochemical Technology Co, Ltd.), ammonium nitrate (NH_4NO_3 , Shanghai Aladdin Biochemical Technology Co. Ltd.), furfuryl alcohol (FA, 99%, Shanghai Aladdin Biochemical Technology Co. Ltd.).

Mesoporous silica (MS, 50 nm) were prepared by a modified Stöber Method as reported in the literature.¹

1.2 Synthesis

1.2.1 Synthesis of zeolites with varied $\text{TBA}^+/\text{TEA}^+$ ratios

The zeolites were synthesized with varied $\text{TBA}^+/\text{TEA}^+$ molar ratios via a simple hydrothermal crystallization method. The initial gel molar composition was $1\text{SiO}_2: 0.01\text{Al}_2\text{O}_3: (0.30-x)\text{TBAOH}: x\text{TEAOH}: 0.04\text{Na}_2\text{O}: 4\text{EtOH}: 20\text{H}_2\text{O}$ ($x=0, 0.01, 0.03, 0.05, 0.07, 0.10$ and 0.15 , the ethanol originates from the hydrolysis of TEOS). In a 50 mL capacity Teflon-lined autoclave, 585 μL 0.1 g/mL NaCl was added to 3.45 mL deionized water under stirring before 27.5 mg NaAlO_2 was dissolved in the solution. Next, a certain amount of TBAOH and TEAOH were added to the solution with stirring. Finally, 3.75 mL TEOS was mixed in the solution and was stirred for 2 h at room temperature until completely hydrolyzed. Afterward, the mixture was hydrothermal and crystallized at 433 K for 72 h in the Teflon-lined stainless-steel autoclave. After crystallization, the crystalline product was recovered by filtration, washed with deionized water three times, and dried overnight at 353 K. The obtained sample was calcined in the flowing air at 823 K for 6 h with a temperature ramping rate of 2 K min^{-1} .

1.2.2 Synthesis of zeolites with varied Si/Al ratios

The zeolites were synthesized with varied Si/Al molar ratios. The initial gel molar composition was $1\text{SiO}_2: n\text{Al}_2\text{O}_3: 0.25\text{TBAOH}: 0.05\text{TEAOH}: 0.04\text{Na}_2\text{O}: 4\text{EtOH}: 20\text{H}_2\text{O}$ ($n=0, 0.0025, 0.005, 0.0067, 0.01, 0.02, 0.04$ and 0.05). Details were identical to that described above.

1.2.3 Synthesis of zeolites with different crystallization temperatures

The zeolites were synthesized at other temperatures. The initial gel molar composition was $1\text{SiO}_2: 0.01\text{Al}_2\text{O}_3: 0.25\text{TBAOH}: 0.05\text{TEAOH}: 0.04\text{Na}_2\text{O}: 4\text{EtOH}: 20\text{H}_2\text{O}$. A series of RA-ZSM-5-50 were synthesized at 293 K, 413 K, 433 K and 453 K, respectively. The preparations were the same as described above except that a different temperature was used for the synthesis.

1.2.4 Synthesis of zeolites with other aluminum and silicon sources

The zeolites were synthesized with other aluminum and silicon sources. The initial gel molar composition was 1SiO₂: 0.01Al₂O₃: 0.25TBAOH: 0.05TEAOH: 0.04Na₂O: 4EtOH: 20H₂O. A series of RA-ZSM-5-50 was synthesized from Si gel, Ludox, MS, Al(i-PrO)₃, Al(OH)₃, Al₂(SO₄)₃ and AlCl₃, respectively. The same procedure was used except for the replacement of other aluminum and silicon sources, respectively.

1.2.5 Synthesis of Con-ZSM-5-50 zeolite

Con-ZSM-5-50 were synthesized hydrothermally with TPAOH. The initial gel molar composition was 1SiO₂: 0.01Al₂O₃: 0.1TPAOH: 0.04Na₂O: 25 H₂O: 4EtOH. In a typical synthesis, 1 g TPAOH and 0.038 g NaOH were dissolved in 8 g deionized water before 0.055 g NaAlO₂ was added to the solution, followed by homogenizing for 5 min under stirring. Then, 4.19 g TEOS was added to the above solution and continuously stirred at room temperature for 2 h. Hydrothermal crystallization of the obtained mixture was conducted statically in Teflon-lined autoclaves (50 mL) at 180 °C for 48 h. The solid products were collected by vacuum filtration and washed with deionized water and dried overnight at 80 °C.

1.2.6 Crystallization process tracking

A series of solid products were taken by quenching crystallization at varied timespans during the crystallization process, and the isolated, as-synthesized samples were analyzed.

1.2.7 Synthesis of H-type samples

To prepare H-type zeolites, 1 g zeolites were subjected to ion exchange in 50 mL 1.0 M NH₄NO₃ solution at 353 K, and vigorously stirred for 4 h. Subsequently, the obtained product was washed three times with deionized water. Finally, the powder was dried and calcined in a muffle furnace in the air for 6 h at a temperature of 823 K after heating with a ramp of 2 K min⁻¹. The ion exchange and calcination processes were repeated three times.

1.3 Characterization

X-ray diffraction (XRD) patterns were operated using a D8 ADVANCE X-ray diffractometer with Cu K α radiation ($\lambda = 0.15406$ nm), with a tube current of 40 mA and a voltage of 40 kV at a scan rate of 0.05 °/s. Taking the zeolite sample with the largest sum peak heights of the five major peaks at $2\theta = 23.1, 23.2, 23.6, 23.9,$ and 24.3° as a reference and assuming that it had a crystallinity of 100%, the relative crystallinity of other zeolite samples was then estimated by comparing their diffraction peak intensity in this range with that of the reference sample.² Scanning electron microscopy (SEM) images were taken with an S4800 electron microscope operating at 5 kV to observe the morphology. Transmission electron microscopy (TEM) experiments were conducted on a Talos-F200S STEM/EDS electron microscope operated at 200 kV. The samples were first dispersed in ethanol and then collected using copper grids covered with carbon films for analysis. Nitrogen adsorption and desorption isotherms of the samples were measured using a Micromeritics ASAP 2020M system at 77 K. Before the measurements, the samples were outgassed at 373 K in a vacuum (1 mbar) for 12 h. The BET surface area was determined by a multipoint BET method using the adsorption data in a relative pressure (P/P_0) range of 0.05-0.3. The calculation from the adsorption branch of the nitrogen isotherms with Barrett-Joyner-Halenda (BJH) method was used to determine the pore sizes. Fourier transform infrared (FT-IR) spectra were obtained on a Nicolet iS50 FT-IR infrared spectrometer. Solid-state Magic-Angle Spinning Nuclear Magnetic Resonance (MAS NMR) spectrum was tracked on a Bruker AVANCE-III 400 spectrometer with a magnetic field intensity of 9.39 T and using a 3.2 mm probe with a spinning rate of 10 kHz. Raman spectra were conducted on a Renishaw InVia Raman spectrometer under visible excitation at 532 nm. The

experiments of temperature-programmed desorption of ammonia (NH₃-TPD) were performed on an AutoChem II 2920 chemisorption analyzer. The sample was purged with He at 500 °C for 1 h to eliminate the physically absorbed ammonia. The NH₃-TPD profile was recorded in flowing He at a heating rate of 10 °C/min from 100 to 700 °C. X-ray photoelectron spectroscopy (XPS) measurements were carried out with an ULVAC-PHI PHI Quantera II system, using a monochromated Al-K α X-ray source, and all spectra were calibrated to a C 1s peak position of 284.8 eV. The distribution of chromophores in zeolites was characterized by a confocal laser scanning microscope (ZEISS LSM 980) with excitation laser sources.

1.4 Catalytic Evaluation

1.4.1 Oligomerization of furfuryl alcohol (FA)

Furfuryl alcohol (FA) oligomerization was used to evaluate the mass transfer performance of zeolite.^{3,4} Typically, H-type ZSM-5 (5 mg) was exposed to 5 mL FA solution (0.008% by volume) for different times, then rapidly collected by vacuum filtration and dried away from light. The samples were then monitored by focusing on the surface of the bottom by ZEISS LSM 980 with excitation laser sources (532 nm). Before the experiments, to avoid residual fluorescence, the crystals were activated at 500 °C (2 °C/min) for 12 h in static air, and the absence of residual fluorescence was verified on individual crystals. All experiments were performed at room temperature.

1.4.2 Methanol-to-olefins (MTO) reaction

The MTO reaction used a fixed-bed quartz tube reactor, H-form zeolite catalysts, and a reaction temperature of 480 °C. The catalysts were pressed and sieved (40-60 mesh) and then two plugs of quartz wool were used to support the catalyst bed (0.2 g) and the reaction temperature was monitored by a K-type thermocouple inserted into the quartz tube. Prior to the reaction, the catalyst bed was activated in situ at 500 °C for 1 h under N₂ (30 mL min⁻¹) flow and then cooled to 480 °C. Methanol (99.9% purity) was continuously fed into the reactor at the weight hourly space velocity (WHSV) of 3.6 h⁻¹ by a syringe pump at 8.4 mL min⁻¹ and then mixed with N₂ flow (30 mL min⁻¹) into a homogeneous phase. The effluent was analyzed by an online gas chromatograph (Shimadzu GC2014C) equipped with a flame ionization detector. Methanol conversion (X) is defined as:

$$X = \left[1 - \left(\frac{C_{eff}}{C_{feed}} \right) \right] \times 100\%$$

Where C_{eff} is the carbon-based molar concentration of both methanol and dimethyl ether measured in the effluent and C_{feed} is the concentration of methanol measured in the feed. The selectivity, S_i , of hydrocarbon product i is defined as:

$$S_i = \left(\frac{C_i}{C_{t,eff}} \right) \times 100\%$$

Where C_i is the carbon-based molar concentration of hydrocarbon i measured in the effluent and $C_{t,eff}$ is the total carbon-based molar concentration of hydrocarbons measured in the effluent.

1.5 Structure Stability

For the hydrothermal (HT) stability test, 0.1 g RA-ZSM-5-50 zeolite and 10 mL deionized water were added to the Teflon-lined stainless-steel autoclave (100 mL) and then transferred to undergo static hydrothermal treatment at 180 °C for 7 days.

For the steam thermal (ST) stability test, 0.1 g RA-ZSM-5-50 zeolite was added in a crucible and 5 mL deionized water was dropped into the bottom of the Teflon-lined stainless-steel autoclave

(100 mL), and then the crucible was transferred into the Teflon lining to undergo static heating at 180 °C for 7 days.

2. Supplementary Figures and Tables

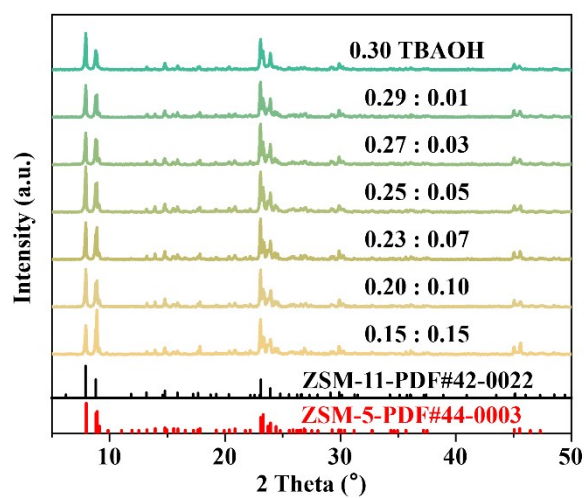


Fig. S1. XRD patterns of as-synthesized samples with varied TBA⁺/TEA⁺ ratios according to (0.30-*x*) TBAOH: *x* TEAOH.

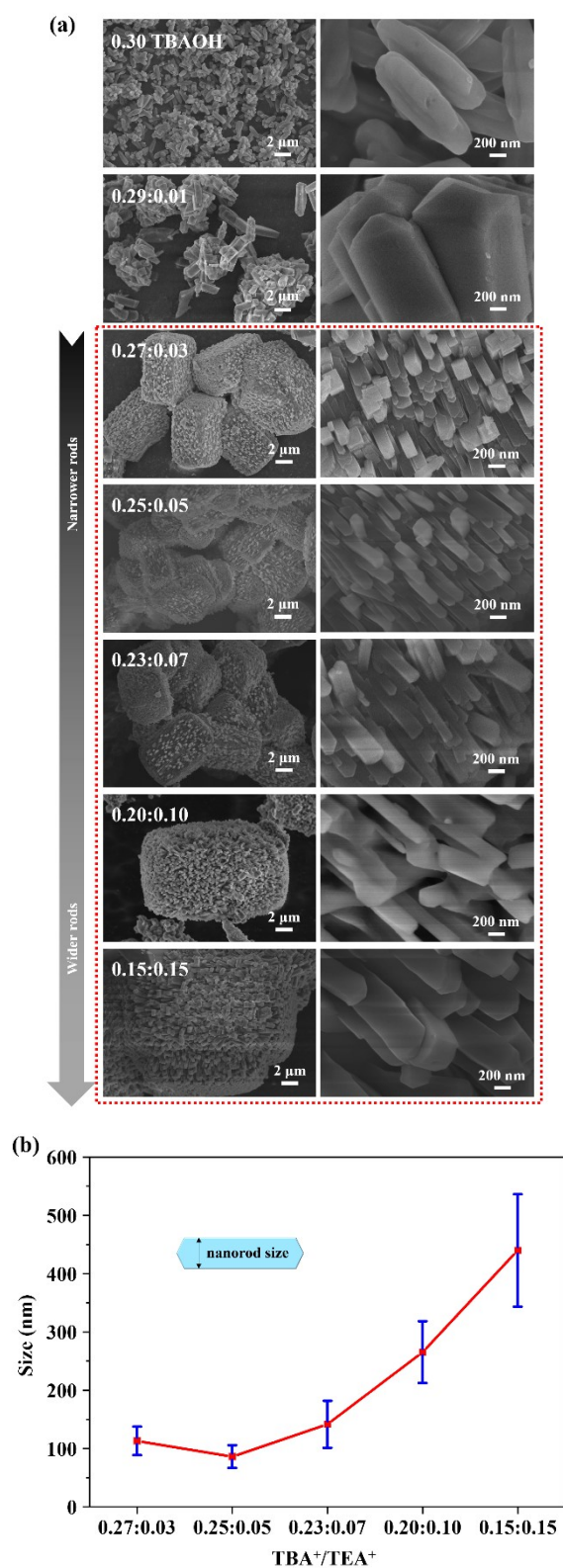


Fig. S2. (a) SEM images of as-synthesized samples with varied TBA⁺/TEA⁺ ratios according to (0.30-*x*) TBAOH: *x* TEAOH and (b) variances curve of nanorod size (evaluated using nanorod widths). Hierarchical zeolite structures with aligned nanorods are formed when the TBA⁺/TEA⁺ molar ratio is below 0.27:0.03, as indicated by the red line.

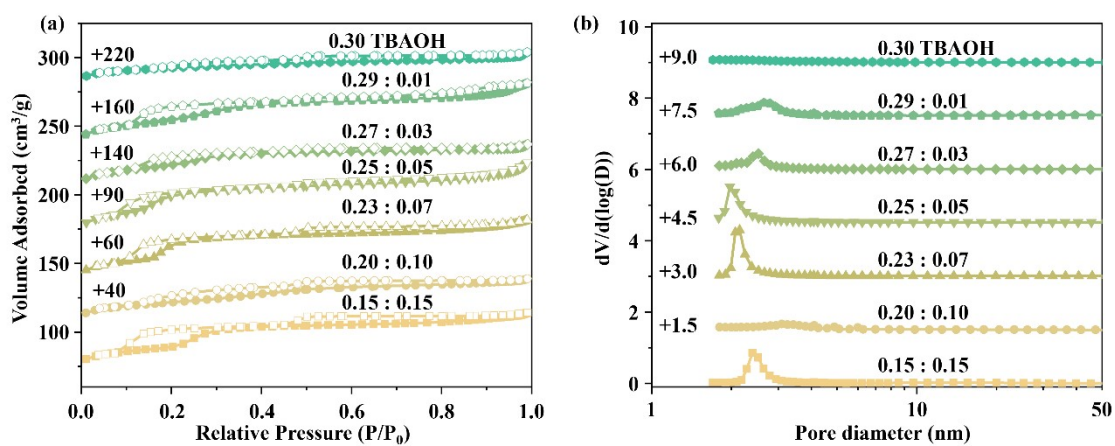


Fig. S3. (a) N₂ physisorption isotherms at 77 K and (b) corresponding pore size distribution (calculated from the adsorption branch of the nitrogen isotherms with BJH method) of as-synthesized samples with varied TBA⁺/TEA⁺ ratios according to (0.30-*x*) TBAOH: *x* TEAOH. For clarity, the curves are displaced along the y-axis by the value given at the start of the curve.

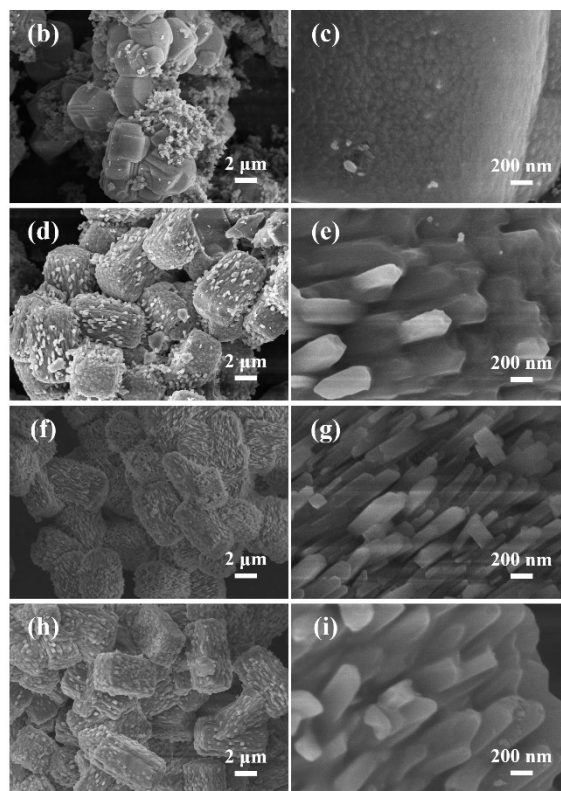
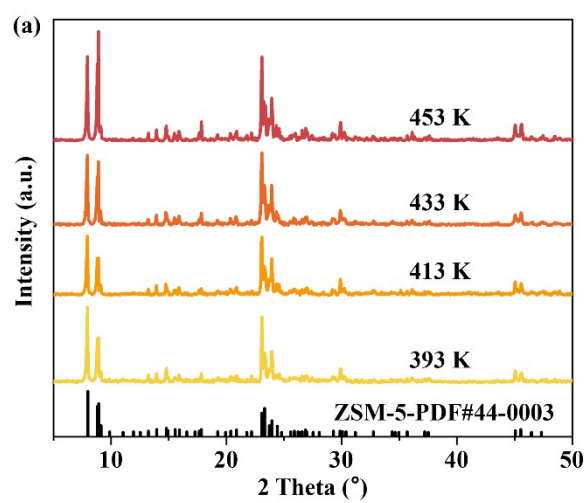


Fig. S4. (a) XRD patterns and (b-i) SEM images of as-synthesized samples of RA-ZSM-5-50 zeolite with varied crystallization temperatures ((b, c) 393 K; (d, e) 413 K; (f, g) 433 K; (h, i) 453 K).

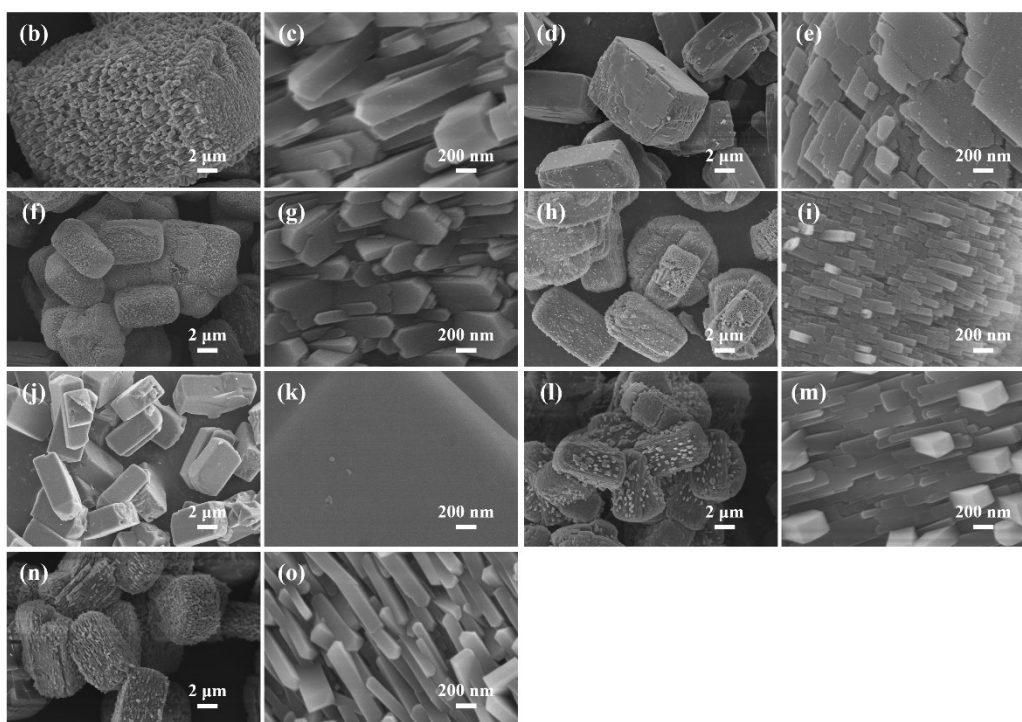
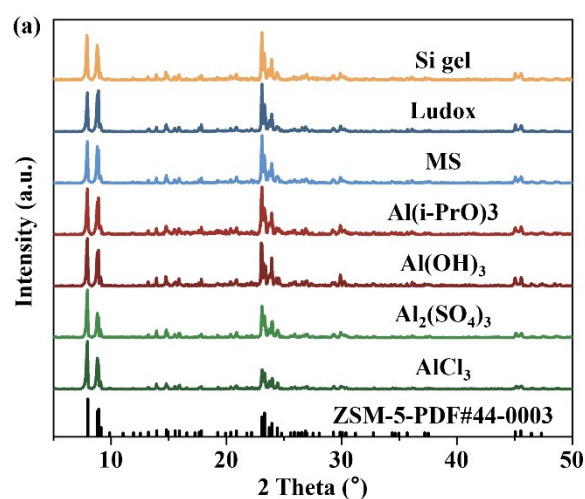


Fig. S5. (a) XRD patterns and (b-o) SEM images of as-synthesized samples synthesized from different aluminum and silicon sources ((b, c) silica gel, (d, e) Ludox, (f, g) mesoporous silica (MS), (h, i) $\text{Al}(\text{i-PrO})_3$, (j, k) $\text{Al}(\text{OH})_3$, (l, m) $\text{Al}_2(\text{SO}_4)_3$, (n, o) AlCl_3). A series of ZSM-5 zeolites having a rod-shaped structure were obtained by utilizing other silicon and aluminum sources, including silica gel, mesoporous silica (MS), $\text{Al}(\text{i-PrO})_3$, $\text{Al}_2(\text{SO}_4)_3$, and AlCl_3 .

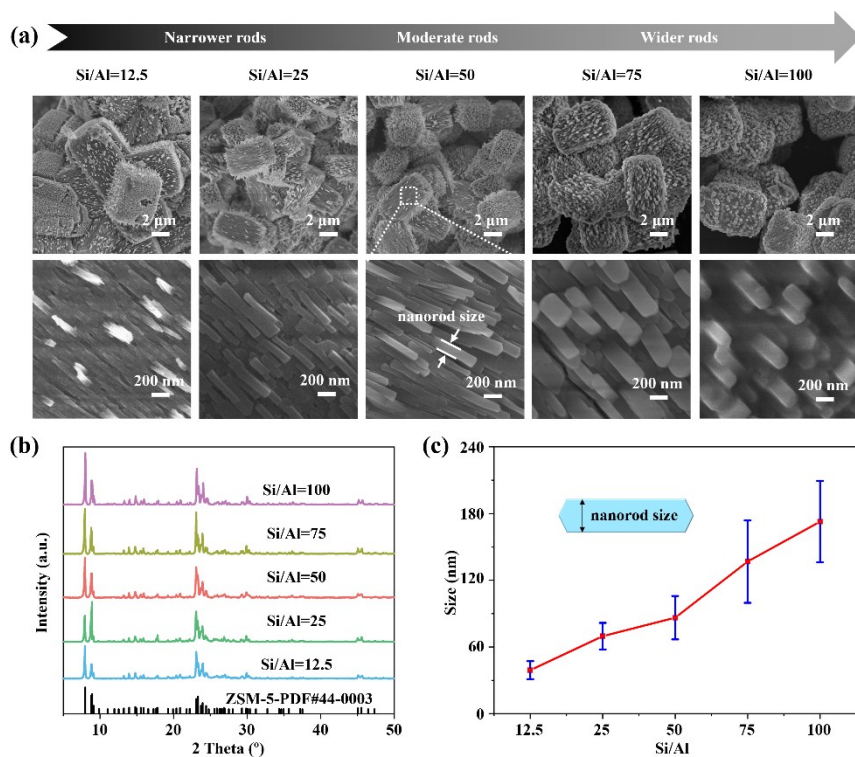


Fig. S6. (a) SEM images (the lower row are magnified images of the surfaces of the micro-block crystal depicted in the upper row), (b) XRD patterns of various Si/Al molar ratios (12.5-100), (c) plot of nanorod size (evaluated using nanorod widths) versus Si/Al molar ratios.

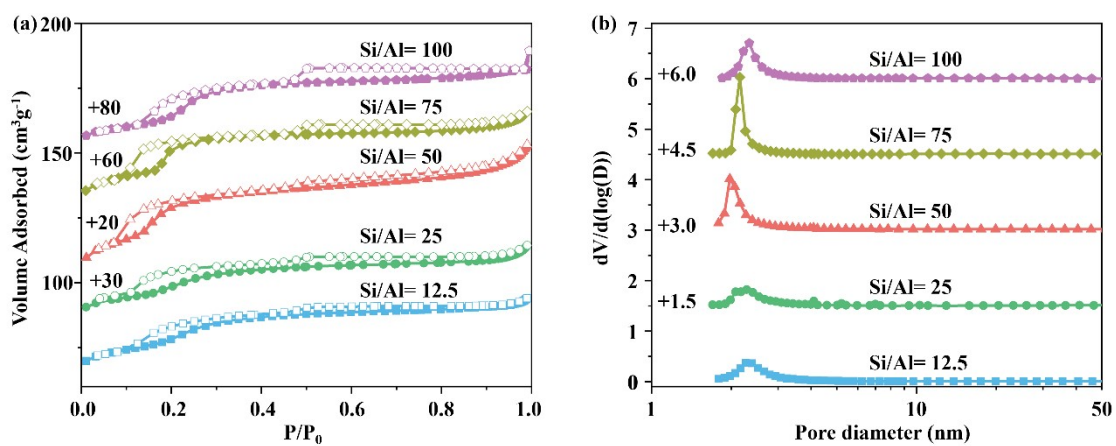


Fig. S7. (a) N₂ physisorption isotherms at 77 K and (b) corresponding pore size distribution (calculated from the adsorption branch of the nitrogen isotherms with BJH method) of as-synthesized samples with varied Si/Al ratios. For clarity, the curves are displaced along the y -axis by the value given at the start of the curve.

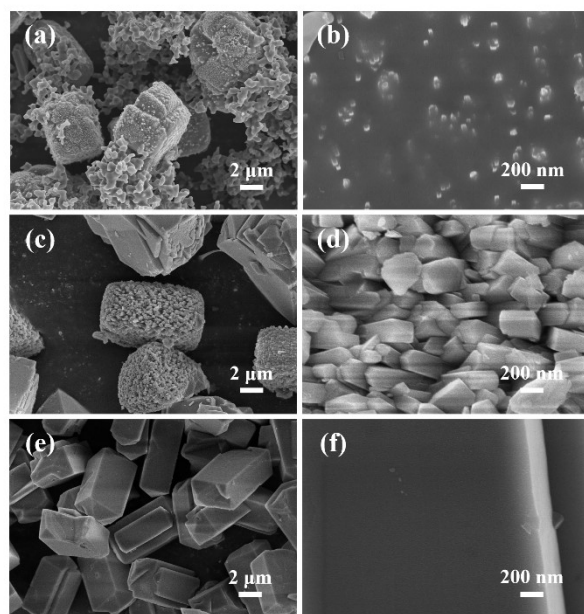


Fig. S8. SEM images of as-synthesized samples with varied Si/Al ratios (a-f: (a, b) 10, (c, d) 200, (e, f) infinite).

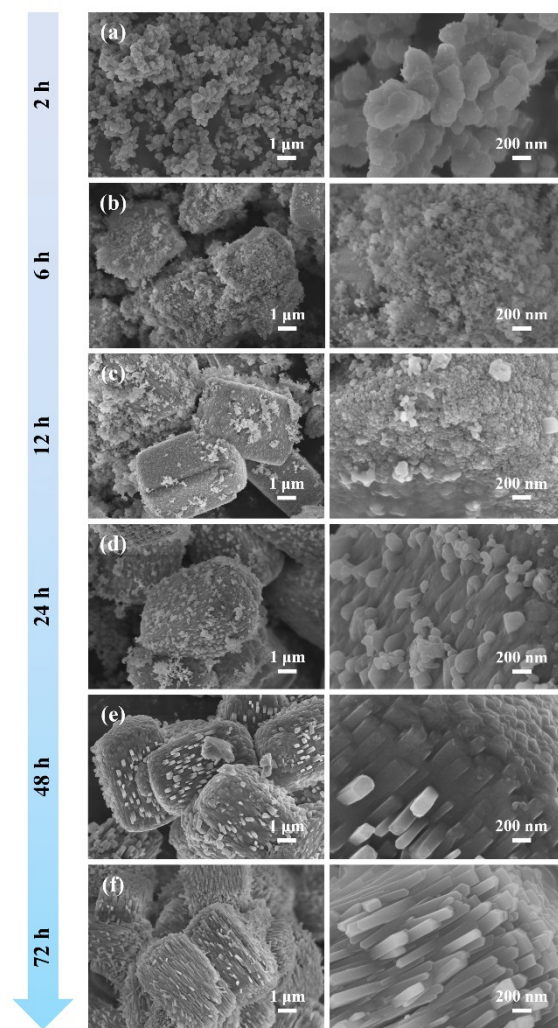


Fig. S9. SEM images of as-synthesized samples with varied crystallization times in different magnifications.

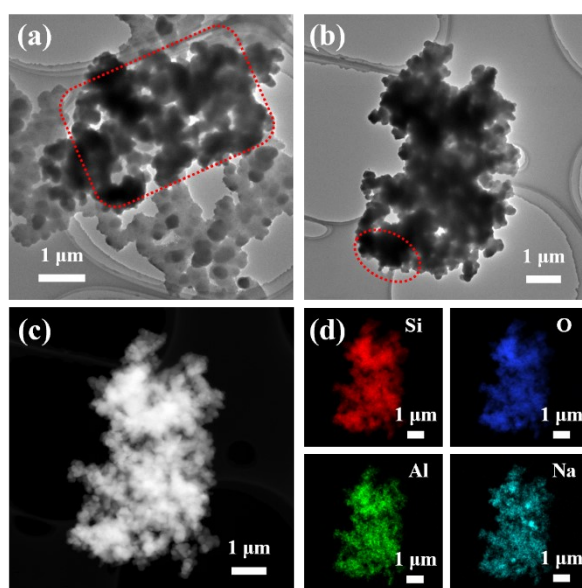


Fig. S10. TEM images, HAADF-STEM image, and corresponding EDS element mapping analysis of the products after a hydrothermal treatment for 2 h.

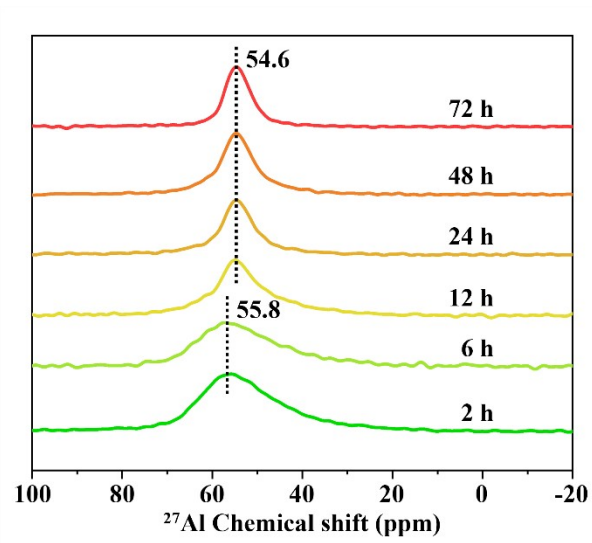


Fig. S11. Solid-state ^{27}Al NMR spectra of samples with varied crystallization time.

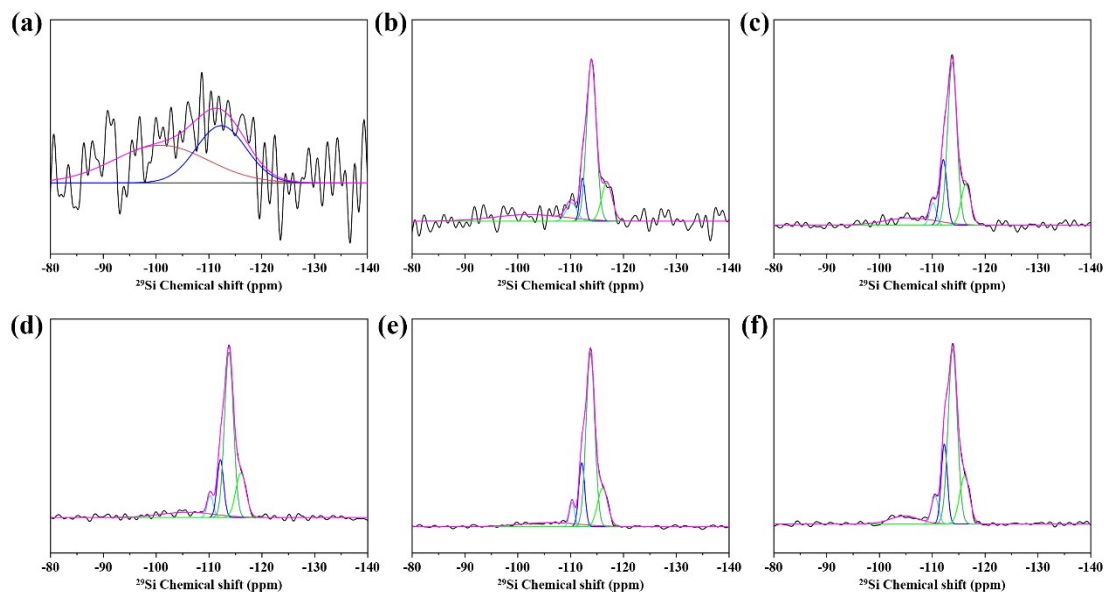


Fig. S12. Solid-state ^{29}Si MAS NMR spectra peak splitting results of as-synthesized samples with varied crystallization time (a-f: (a) 2 h, (b) 6 h, (c) 12 h, (d) 24 h, (e) 48 h, (f) 72 h). The chemical shifts of lower intensities at $-(100-108)$ ppm could be attributed to Q^3 [$\text{Si}(\text{OSi})_3(\text{OH})$], and the stronger intensities at $-(108-120)$ ppm could be assigned to framework [$\text{Si}(\text{OSi})_3(\text{OAl})$] and Q^4 [$\text{Si}(\text{OSi})_4$], as shown in Table S3 and S4.⁵

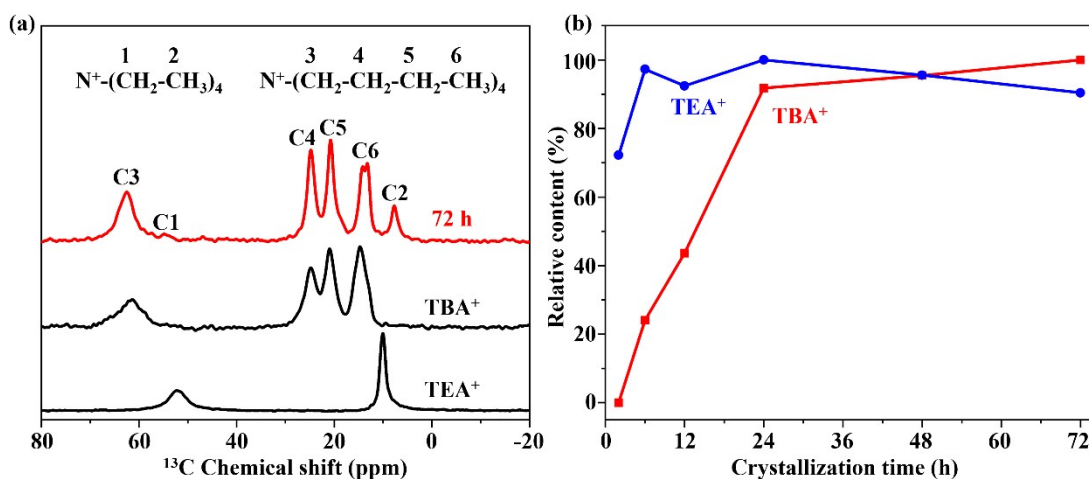


Fig. S13. Solid-state ^{13}C MAS NMR spectra of standard samples. (b) Relative content curves of TEA^+ (blue) and TBA^+ (red). The chemical shifts of the peaks at 7.6 and 53 ppm correspond to TEA^+ , while the peaks at 13.2/14.2, 20.6, 24.7, and 62.2 ppm correspond to TBA^+ . The relative content of TEA^+ (TBA^+) was calculated using the formula $(p_n/p_s) \times 100\%$ according to Fig. 4e, where p_n represents the peak intensity of C2 (average peak intensity of C4, C5, and C6) at different synthesis times, and p_s represents the strongest peak intensity in the entire spectrum.⁶

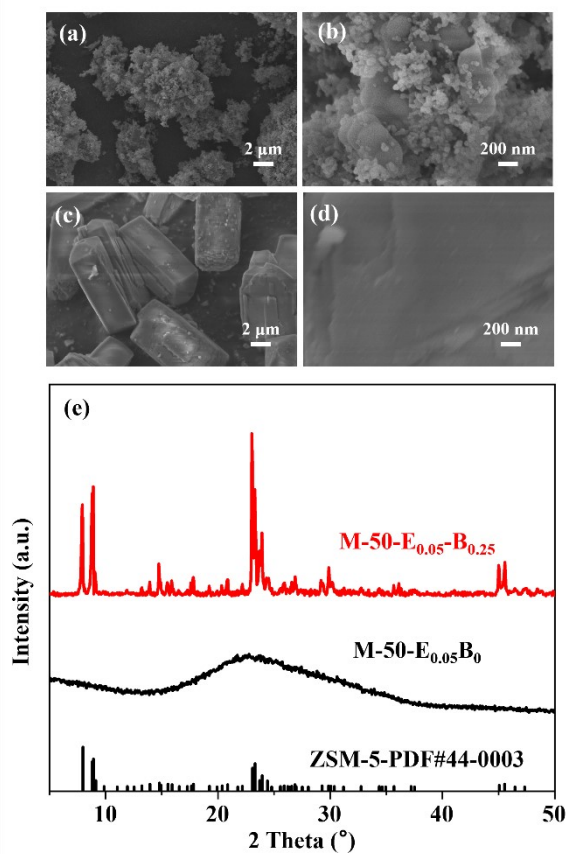


Fig. S14. (a-d) SEM images and (e) XRD patterns of M-50-E_{0.05}B₀ and M-50-E_{0.05}-B_{0.25}. M-50 represents a Si/Al molar ratio of 50; E and B represent TEA⁺/Si and TBA⁺/Si molar ratios, respectively; M-50-E_{0.05}B₀ was prepared from the charge molar ratio of 1SiO₂: 0.01Al₂O₃: 0.04Na₂O: 0.05TEAOH: 20H₂O for 3 d at 433 K. M-50-E_{0.05}-B_{0.25} was prepared in two steps: First, TEAOH was added and the mixture was reacted at 433 K for 3 d; second, TBAOH was added and the reaction was continued at 433 K for another 3 d. The overall molar ratio was 1SiO₂: 0.01Al₂O₃: 0.04Na₂O: 0.25TBAOH: 0.05TEAOH: 20H₂O, which is the same as that of RA-ZSM-5-50.

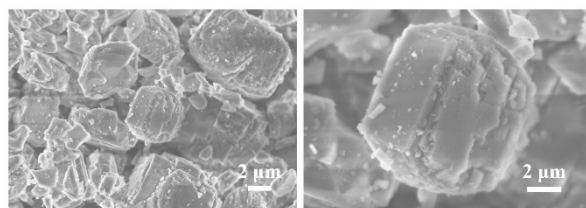


Fig. S15. SEM images of Con-ZSM-5-50 zeolite.

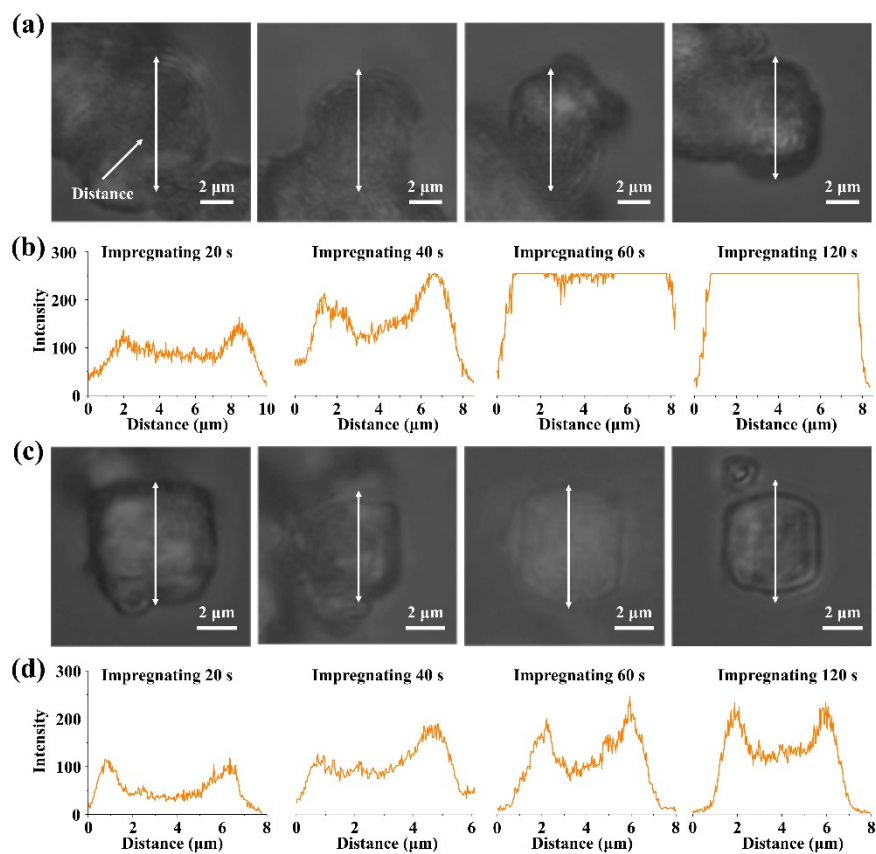


Fig. S16. (a, c) Images of samples with different reaction times and (b, d) corresponding linear distribution curve of fluorescence intensity (the arrow represents the distance).

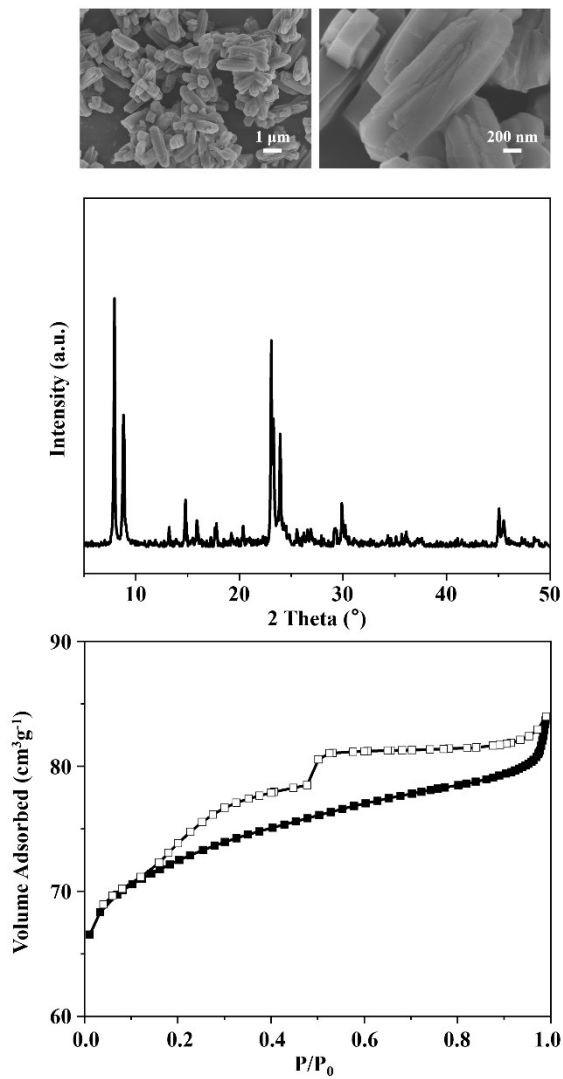


Fig. S17. The SEM images, XRD pattern, and N₂ physisorption isotherms at 77 K of rod-shaped ZSM-11 (R-ZSM-11-50) synthesized with TBAOH as SDA only.

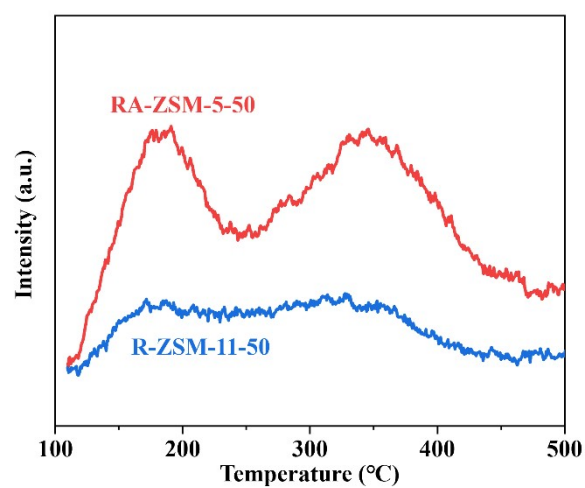


Fig. S18. NH₃-TPD curves of RA-ZSM-5-50 and R-ZSM-11-50.

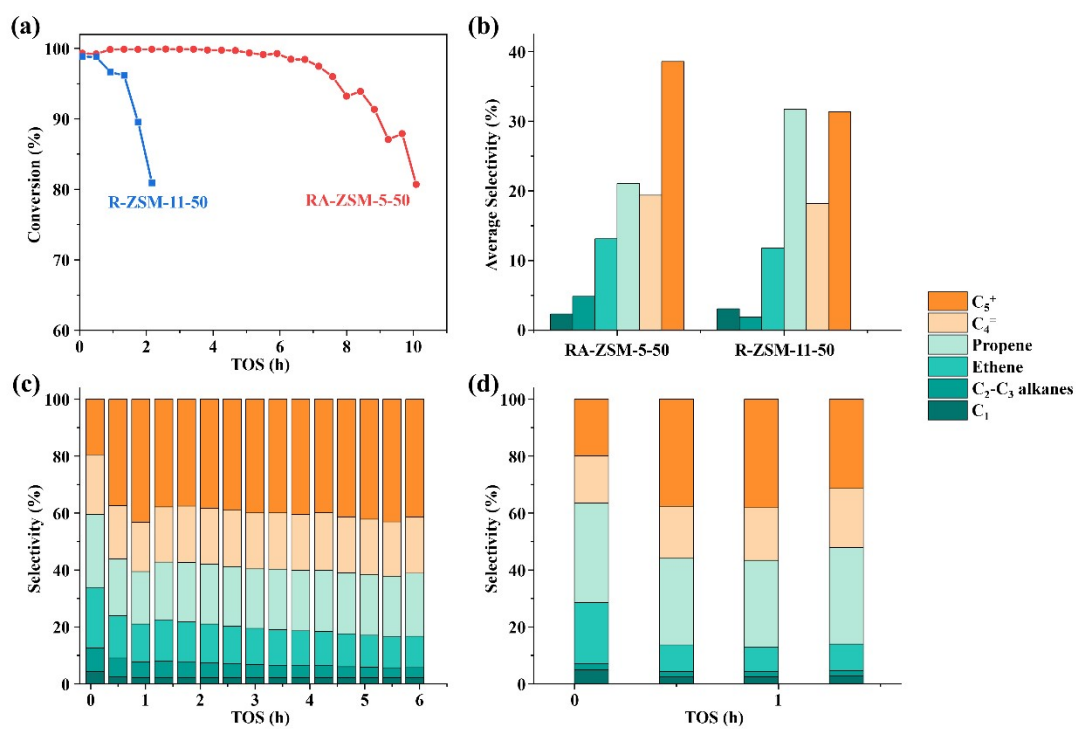


Fig. S19. The results of MTO reactions showing the (a) lifetime, (b) product average selectivity, and (c, d) product selectivity as a function of time on stream (TOS) for the following H-type zeolites: (c) RA-ZSM-5-50, (d) R-ZSM-11-50. All reactions were performed at the weight hourly space velocity (WHSV) of 3.6 h⁻¹.

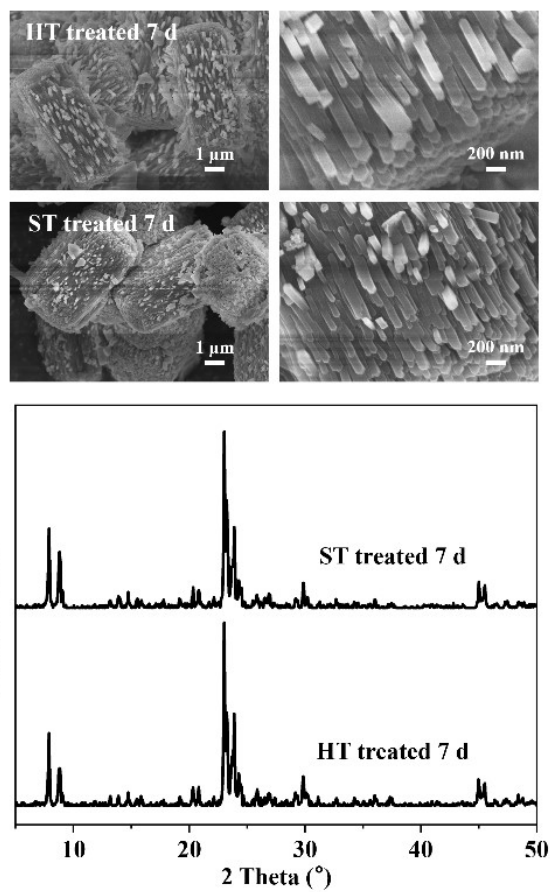


Fig. S20. The SEM images and XRD patterns of RA-ZSM-5-50 zeolite after different treatments.

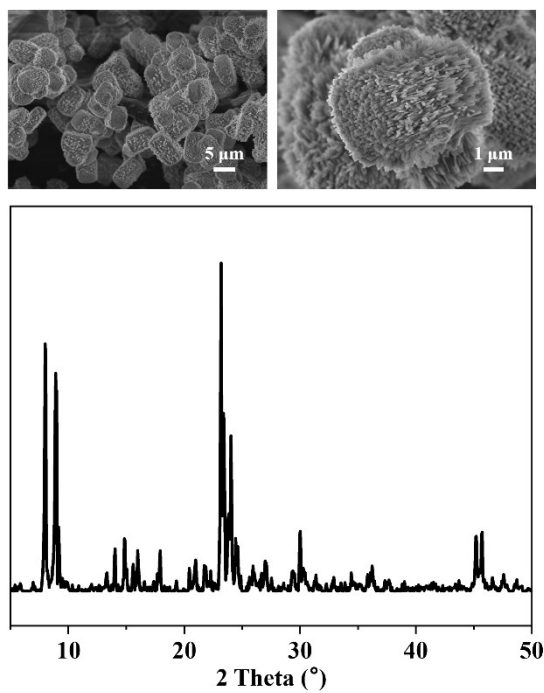


Fig. S21. The SEM images and XRD patterns of RA-ZSM-5-50 zeolite after 12 days of hydrothermal crystallization.

Table S1. Textural properties of calcined samples derived from N₂ physisorption isotherms.

Sample	S _{BET} (m ² g ⁻¹) ^a	S _{ext} (m ² g ⁻¹) ^b	V _{total} (cm ³ g ⁻¹) ^c	V _{micro} (cm ³ g ⁻¹) ^b
ZSM-5-E _{0.15} B _{0.15}	299	150	0.18	0.08
ZSM-5-E _{0.10} B _{0.20}	243	60	0.15	0.10
ZSM-5-E _{0.07} B _{0.23}	332	232	0.19	0.05
ZSM-5-E _{0.05} B _{0.25}	341	215	0.21	0.07
ZSM-5-E _{0.03} B _{0.27}	286	163	0.16	0.07
ZSM-5-E _{0.01} B _{0.29}	295	108	0.19	0.10
ZSM-5-E ₀ B _{0.30}	213	37	0.13	0.10
ZSM-5-SA-12.5	250	166	0.14	0.05
ZSM-5-SA-25	217	107	0.13	0.06
ZSM-5-SA-75	289	194	0.16	0.05
ZSM-5-SA-100	280	277	0.17	0.01

Notes: E and B represent TEA⁺/Si and TBA⁺/Si molar ratio, respectively; SA represent the Si/Al molar ratio.

[a] Calculated using the BET method; [b] Deduced from the *t*-plot method; [c] Inferred from volume adsorbed at P/P₀ = 0.99.

Table S2. Textural, acidity, and Si/Al ratio of samples derived from the results of elemental analysis.

samples	S _{BET} (m ² g ⁻¹) ^a	S _{ext} (m ² g ⁻¹) ^b	V _{total} (cm ³ g ⁻¹) ^c	V _{micro} (cm ³ g ⁻¹) ^b	C _{acid} (μmol/g) ^d		Si/Al ^e
					Weak	Strong	
RA-ZSM-5-50	341	215	0.21	0.07	137	180	47
R-ZSM-11-50	213	37	0.13	0.10	42	51	46

[a] determined by the multi-point BET method. [b] analyzed by *t*-plot method. [c] using the adsorption data at P/P₀ = 0.99. [d] weak and strong acid site density (C_{acid}) measured by NH₃-TPD. [e] calculated based on XPS.

Table S3. Solid state ^{29}Si MAS NMR data of as-synthesized samples with varied crystallization time.

samples	Q ³		Q ⁴		
	Si(OSi) ₃ OH (ppm)	Si(OSi) ₃ (OAl) (ppm)	Si(OSi) ₄ (ppm)		
2 h	-100.9	-	-112.3	-	-
6 h	-102.2	-110.2	-112.3	-113.9	-116.9
12 h	-105.9	-110.1	-112.1	-113.8	-116.3
24 h	-105.9	-110.2	-112.1	-113.7	-116.0
48 h	-106.1	-110.3	-112.1	-113.8	-116.1
72 h	-104.8	-110.5	-112.3	-113.9	-116.1

Table S4. Deconvolution results of the ^{29}Si MAS NMR spectra of as-synthesized samples with varied crystallization time based on the normalized peak areas of the different Si species.

samples	Q ³		Q ⁴		
	Si(OSi) ₃ OH (%)	Si(OSi) ₃ (OAl) (%)	Si(OSi) ₄ (%)		
2 h	55	0	45	0	0
6 h	16	7	8	54	15
12 h	13	5	16	52	14
24 h	10	5	14	54	17
48 h	9	5	14	57	15
72 h	8	6	16	54	16

3. References

- 1 Q. Gao, Y. Xu, D. Wu, Y. Sun and X. Li, *J. Phys. Chem. C*, 2009, **113**, 12753-12758.
- 2 Z. Qin, L. Lakiss, L. Tosheva, J. P. Gilson, A. Vicente, C. Fernandez and V. Valtchev, *Adv. Funct. Mater.*, 2013, **24**, 257-264.
- 3 Z. Ristanovic, J. P. Hofmann, G. De Cremer, A. V. Kubarev, M. Rohnke, F. Meirer, J. Hofkens, M. B. Roeffaers and B. M. Weckhuysen, *J. Am. Chem. Soc.*, 2015, **137**, 6559-68.
- 4 S. Peng, H. Li, W. Liu, J. Yu, Z. Xu, M. Ye and Z. Liu, *Chem. Eng. J.*, 2022, **430**, 132760.
- 5 R. J. Messinger, K. Na, Y. Seo, R. Ryoo and B. F. Chmelka, *Angew. Chem. Int. Ed.*, 2015, **54**, 927-31.
- 6 X. Zhao, S. Zeng, X. Zhang, Q. Deng, X. Li, W. Yu, K. Zhu, S. Xu, J. Liu and L. Han, *Angew. Chem. Int. Ed.*, 2021, **60**, 13959-13968.